

Influence of Calcining Temperature on the Mineralogical and Mechanical Performance of Calcined Impure Kaolinitic Clays in Portland Cement Mortars

Boakye, K, Khorami, M, Saidani, M, Ganjian, E, Dunster, A, Tyrer, M & Ehsani, A

Author post-print (accepted) deposited by Coventry University's Repository

Original citation & hyperlink:

Boakye, K, Khorami, M, Saidani, M, Ganjian, E, Dunster, A, Tyrer, M & Ehsani, A 2024, 'Influence of Calcining Temperature on the Mineralogical and Mechanical Performance of Calcined Impure Kaolinitic Clays in Portland Cement Mortars', *Journal of Materials in Civil Engineering*, vol. 36, no. 4.

<https://dx.doi.org/10.1061/JMCEE7.MTENG-16128>

DOI 10.1061/JMCEE7.MTENG-16128

ISSN 0899-1561

Publisher: ACSE

This material may be downloaded for personal use only. Any other use requires prior permission of the American Society of Civil Engineers. This material may be found at <https://ascelibrary.org/doi/10.1061/JMCEE7.MTENG-16128>

This document is the author's post-print version, incorporating any revisions agreed during the peer-review process. Some differences between the published version and this version may remain and you are advised to consult the published version if you wish to cite from it.

1 **Influence of calcining temperature on the mineralogical and mechanical performance of**
2 **calcined impure kaolinitic clays in Portland cement mortars**

3 Kwabena Boakye¹; Morteza Khorami²; Messaoud Saidani³; Eshmaiel Ganjian⁴; Andrew Dunster⁵;
4 Mark Tyrer⁶ and Ahmad Ehsani⁷
5

6 ¹ Postgraduate Researcher, School of Energy, Construction & Environment, Faculty of Engineering &
7 Computing, Coventry University, Coventry, U.K. ORCID: <https://orcid.org/0000-0001-5290-0332>. Email:
8 boakyek4@uni.coventry.ac.uk

9 ² Associate Professor, Civil Engineering and Structural Design, School of Energy, Construction & Environment,
10 Faculty of Engineering & Computing, Coventry University, Coventry, U.K (Corresponding Author). ORCID:
11 <https://orcid.org/0000-0002-1656-8704>. Email: aa8186@coventry.ac.uk

12 ³ Associate Professor, School of Energy, Construction & Environment, Faculty of Engineering & Computing,
13 Coventry University, Coventry, U.K. Email: cbx086@coventry.ac.uk

14 ⁴ Professor, Civil Engineering Materials, Concrete Corrosion Tech Ltd., Birmingham, United Kingdom. Email:
15 eganjian@yahoo.co.uk

16 ⁵ Principal Consultant, Building Research Establishment (BRE), UK. Email: andrew.dunster@bregroup.com

17 ⁶ Professor, Geomaterials and Geochemistry, Institute of Advanced Study ((Collegium Basilea), 4053 Basel,
18 Switzerland. Email: m.tyrer@mtyrer.net

19 ⁷ Research Scientist, Indo-UK Centre for Environmental Research and Innovation, University of Greenwich, UK.
20 Email: a.ehsani@greenwich.ac.uk
21

22 **Abstract**

23 In this work, the effects of calcination temperatures ranging from 600 to 1000 °C on the
24 changes in mineralogical phases and mechanical characteristics of calcined impure kaolinite
25 clay blended cement mortars were investigated. The impact of calcining temperature on
26 pozzolanic activity of impure kaolinite clay was evaluated using direct and indirect methods.
27 The findings demonstrated that at 700 °C, kaolinite changed from a crystalline to an amorphous
28 metakaolin phase. Specific surface, water demand and setting time of the blended cements
29 decreased as calcining temperature increased. The compressive strengths of blended cement
30 mortar containing low-grade clay calcined at 700 °C, 800 °C and 900 °C were found to be
31 greater than that of 600 °C and 1000 °C. Based on the results of pozzolanic reactivity
32 evaluations and compressive strength development, the most effective calcining temperature
33 was shown to be between 800 °C and 900 °C.
34

35 **Author Keywords:** calcined clay; low-grade kaolinitic clays; mineralogical properties;
36 calcining temperature; pozzolanic reactivity

37 **Introduction**

38 One of the most realistic and practical ways to significantly deal with the SCM availability
39 challenges, while reducing the environmental consequences of cement manufacture, has been
40 found to be the adoption of clays with high amounts of kaolinite for the preparation of SCMs for
41 construction purposes (Antoni et al., 2012). This is in part due to their widespread availability
42 in many countries. Again, the utilisation of these clays and other geologic materials in
43 cementitious systems could significantly reduce the reliance of GGBS and fly ashes for composite
44 cement production (Msinjili et al., 2019, Scrivener et al., 2018). However, the adoption and
45 general use of calcined impure clays in cement replacement is restricted, in part because of a lack
46 of understanding of the factors that define their pozzolanic reactivity and consequently, concrete
47 properties.

48

49 The three main clay minerals that are mostly present in most of clays studied by researchers are
50 kaolinite, illite, and smectites. In several reports, the highest and most efficient pozzolanic
51 activities are found in clays with appreciable levels of kaolinite minerals, which also require the
52 minimum calcining temperatures (based on their crystallinity) for the highest performance
53 (Snellings et al., 2016). This is largely related to the number and placement of hydroxyl groups
54 in kaolinite, which supports amorphization during heat treatment, and the existence of
55 considerable amounts of energetically reactive five-coordinated Al in metakaolin (Msinjili et al.,
56 2019, Scrivener et al., 2018). However, it has been demonstrated that illite and smectites can also
57 exhibit pozzolanic properties after being heat-treated at the appropriate temperatures (800 – 950
58 °C). Compared to kaolinite, these minerals often exhibit lower abundance of five-coordinated Al
59 (Lothenbach et al., 2011). Furthermore, kaolinite has a higher rate of dissolution in alkaline
60 solutions than smectites, which have an octahedral sheet firmly placed between two tetrahedral
61 sheets (Danner et al., 2018). Likewise, comparable structural features of clay minerals may be

62 responsible for the disparity in the degree of reactivity between illites and smectites and
63 metakaolin, after heat treatment (Arslan et al., 2020, Karatas et al., 2020).

64

65 The particle size and mineralogical makeup of clays obtained from various places can occasionally
66 have an impact on the level of pozzolanic activity (Zheng et al., 2022). Recent years have seen
67 some investigations by researchers on the use of clays with low kaolinite levels in Portland cement
68 mortar and concrete (Dixit et al., 2020, Dixit et al., 2021, Du and Pang, 2018, Zheng et al.,
69 2022, Zhou et al., 2017). Although majority of studies base their clay classification on their
70 kaolinite content, there is no consensus on what constitutes high- or low-grade clays. Some
71 researchers have suggested that kaolinite levels above 40% can typically be referred to as high
72 grade, using a firing temperature of 700 – 900 °C. In recent times, the focus of calcined clay
73 research has shifted to clays with lower content of kaolin due to the high cost and unavailability
74 of high-grade kaolinitic clays in every region. Investigating the ideal temperature at which the
75 maximum reactivity can be achieved in low kaolinitic clays, and the optimum Portland cement
76 substitution is therefore worthwhile.

77

78 The reactivity of calcined clay in cementitious matrices is largely due to dehydroxylation of
79 kaolinite, which is also related to the mineralogical composition of the clay and calcining
80 conditions, thus, temperature and time (Kaminskas et al., 2023, Tironi et al., 2017). Although
81 low-grade kaolinitic clays contain a variety of minerals, both reactive or inert minerals, they
82 have been found to possess some level of pozzolanic reactivity after calcining at an appropriate
83 temperature (Taylor-Lange et al., 2015). The selected calcining temperature is based on the
84 desired properties of the resultant calcined clay. 600 °C is typically considered to be a good
85 temperature when the aim is to increase the reactivity of the clay (He et al., 1994). However, if
86 the goal compressive strength of regular concrete or mortar is desired, calcining at 800 °C may

87 be appropriate, amidst other factors (Kang et al., 2022). Again, calcining temperature may also
88 affect some physical properties of the clay including shape, size and surface area, which
89 ultimately influences the compressive strength and durability of concrete (Ferreiro et al., 2017).

90

91 There have been investigations on the application of impure kaolinitic clays as SCM in the last
92 few years. Alujas et al. (2015) studied the pozzolanicity of impure clays and reported that, clays
93 possessing a kaolinite content of about 40% or more perform much better in terms of their
94 reactivity as compared to clays containing kaolinite composition of less than 40%. The
95 suitability of excavated waste London clay, obtained from construction site, as an SCM was
96 evaluated by Zhou et al. (2017). The waste clay was thermally activated at temperatures
97 between 600 °C and 1000 °C. The calcined clay showed that a relatively higher pozzolanic
98 reactivity at temperatures beyond 700 °C. This significantly reflected in the mechanical
99 properties of the resultant concrete, outperforming clays calcined at lower temperatures. Lower
100 carbon footprint was recorded for concrete containing calcined clay than plain concrete. The
101 pozzolanicity of heat-treated dredged soils, as reported by Snelling et al. (2016), indicated a
102 higher pozzolanic reactivity as compared to fly ash and slightly lower than results obtained for
103 metakaolin. Danner et al. (2018) concluded that, the incorporation of calcined clays in
104 sustainable concrete production has the potential to significantly reduce the release of
105 deleterious gases to the environment and overall production cost. The influence of calcining
106 temperature on the hydration and mechanical properties of Tunisian clays was experimented
107 by Nawel et al. (2020). Pozzolanic reactivity was found to be at its highest when the clay was
108 calcined at 600 °C. Du and Pang (2018) also studied the properties of marine clay (containing
109 a kaolinite content of 20%) after heat treatment. A high strength activity index of 0.9 was
110 achieved for clays calcined at 600 °C.

111

112 This work has examined how low-grade clay, which contains 17% kaolinite, changed in terms of
113 its physical and mineralogical properties as a result of calcination temperature. Utilizing
114 portlandite consumption, Frattini and compressive strength test results, the pozzolanic reactivity
115 of the calcined clay was examined. X-ray diffraction (XRD) and differential scanning calorimetric
116 (DSC) studies were conducted on the raw clay and blended cements. Additionally, the optimum
117 calcination temperature was established. The impacts of calcined clay as an SCM on the
118 characteristics of mortar were also investigated. The findings of this study will offer a theoretical
119 underpinning for its widespread application as well as a roadmap for expanded usage of impure
120 clays as supplementary cementitious materials in regions where there are no pure kaolinite
121 reserves.

122

123 **Materials and Methodology**

124 ***Materials***

125 Clay used for study was sampled from a deposit located in Buckinghamshire, England. Portland
126 cement CEM I 52.5 N conforming to BS EN 197-1 was the main binder used for the preparation
127 of blended cement pastes and mortars. The Portland cement had a specific surface area of 410
128 m²/kg. Fine aggregate, conforming to BS 4550: Part 6 was supplied by local dealers.

129

130 **Methodology**

131 ***Calcined clay***

132 The clay sample was dried in a laboratory oven at 105 °C for 24 h. It was then milled in a
133 portable quartz crusher for 2 minutes into powder (150 μm) and calcined for 2 hours in a muffle
134 furnace at varying temperatures of 600 °C, 700 °C, 800 °C, 900 °C and 1000 °C using a heating
135 rate of 10 °C /min. The clay removed after calcination and left on a laboratory bench to cool to
136 an ambient temperature in air for approximately 2 hours. The calcined clay was further ground

137 and sieved through a 75 μm sieve. The percentage passing (about 95%) was used and the rest
138 discarded.

139

140 X-ray diffraction (XRD) technique was used for phase identification of raw and hydrated
141 cement samples.. Thermal analysis (TG/DSC) was also conducted between 30 $^{\circ}\text{C}$ and 1000 $^{\circ}\text{C}$,
142 utilising a heating rate of 20 $^{\circ}\text{C}/\text{min}$. Nitrogen gas with a flow rate of 20 ml/min was flashed in
143 the heating chamber to reduce the possibility of carbonation. The laser diffraction method was
144 used in studying the particle size distribution (PSD) of the calcined clay and blended cements.
145 Ultrasound was employed to aid the disintegration of the sample in the water inside the sample
146 vessel. Setting times and water demand was conducted according to methods specified by
147 ASTM C191-21.

148

149 *Pozzolanic reactivity*

150 The Frattini test, portlandite consumption test, strength activity index and the relative strength
151 index were the methods employed to measure pozzolanic reactivity. Blended cement was
152 prepared by partially replacing 20% by weight of CEM-I cement with calcined clay having
153 different calcination temperatures (600 $^{\circ}\text{C}$, 700 $^{\circ}\text{C}$, 800 $^{\circ}\text{C}$, 900 $^{\circ}\text{C}$ and 1000 $^{\circ}\text{C}$). According to
154 the procedures outlined in BS EN 196-1:2016, mortar cubes of 50 x 50 x 50 mm were prepared
155 in triplicate, using a water-to-binder ratio of 0.5 and binder/sand ratio of 1:3. After curing the
156 mortar cubes in water for a period of 3, 7, 28 and 91 days, their individual compressive
157 strengths were determined by crushing in a compressive strength testing machine and the
158 results calculated. The RSI technique is predicated on the idea that the projected drop in
159 strength will be directly related to the SCM percentage in the absence of pozzolanic
160 activity. The RSI is calculated using the formula shown in equation 1.

$$161 \quad RSI = RP - (100 - S) \quad (1)$$

162 Where RP (real potential) is the ratio between the compressive strength of the composite
163 cement and the reference cement (same calculation as strength activity index). S is the quantity
164 (in mass-percentage) of pozzolan in the mixture.

165

166 **Results and Discussions**

167 *Characterisation of calcined clay*

168 Figure 1 is a presentation the PSD of the calcined clays used in this research. As seen, the
169 calcined clay samples showed similar and close trend of particle size distributions with an
170 average d_{10} of $1.02 \mu\text{m}$, a d_{50} of $9.08 \mu\text{m}$ and a d_{90} of $51 \mu\text{m}$. Clay calcined at 900°C was
171 found to have the highest particle fineness whereas 800°C and 1000°C obtained the least in
172 the group.

173

174 BET surface area of the calcined clay samples decreased ($20 \text{ m}^2/\text{g}$, $18.6 \text{ m}^2/\text{g}$, $12.6 \text{ m}^2/\text{g}$, 7.4
175 m^2/g and $5.6 \text{ m}^2/\text{g}$) as the calcining temperature increased from $600 - 1000^\circ\text{C}$ respectively.

176 The obvious decrease in surface area was seen between 700 and 800°C (18.6 to $12.6 \text{ m}^2/\text{g}$).

177 From Section 3.2, the transformation of illite and smectite was completed at 800°C and may
178 undergo further structural changes beyond 850°C as confirmed by other studies. The reduction
179 in surface area could be due to the changes in illite and smectite at 800°C .

180 Density measurements of the calcined clay also varied between $2.6 \text{ g}/\text{cm}^3$ and $2.9 \text{ g}/\text{cm}^3$ in a
181 slightly decreasing order, as calcination temperature increased. This is due to the evaporation
182 of combined water, reduction in weight, as shown by the TG measurement in Figure 5 and
183 consequently a decrease in density as temperature increased.

184

185 A plot of the setting time and water demand is shown in Figure 2. The incorporation of calcined
186 clay caused a significant increase in setting time. Initial and final setting times increased by

187 19% and 22.2% respectively in blended cement containing 600 °C calcined clay. However,
188 varying calcining temperatures impacted setting times differently. As temperature of
189 calcination increased between 600 °C and 1000 °C, setting time decreased. Similarly, water
190 demand was observed to decrease with increasing calcining temperature.

191

192 *Effect of calcination of microstructural changes*

193 Figure 3 is the XRD analysis of the clay calcined at different temperatures. The major minerals
194 identified in the clay by x-ray diffraction analysis were quartz, kaolinite, illite and smectite, as
195 shown in Figure 3. The crystallinity of the clay is slowly reduced, giving way to the emergence
196 of amorphous phases, after calcining at varying temperatures. Dehydroxylation appears to
197 begin at 600 °C, causing the corresponding peak to fade. With the increase in temperature, the
198 peaks corresponding to illite and montmorillonite were found to decrease, confirming
199 observations reported by other researchers. There was a low amount of spinel phase observed
200 when the temperature was increased to 1000 °C. This could indicate the beginning of re-
201 crystallization of the amorphous phases.

202

203 The thermogravimetric study of the clay and calcined clays are seen in Figures 4 and 5. There
204 is an appreciable mass loss of about 1.71% between 50 – 100 °C which is usually the dissipation
205 of water causing dehydration. Dehydroxylation of the clay minerals occurs between 400 and
206 700 °C. As temperature is increased, there is a mass loss of 2.31% and a wider exothermic peak
207 shows up between 458 °C and 531 °C which typically corresponds to the dehydroxylation (the
208 removal of structural water molecules) of kaolinite and the formation of metakaolinite. The
209 amount of kaolinite in this clay can be estimated to be 17% based on this mass loss and the
210 molecular weights of kaolinite and water. There also appears to be two small peaks overlapping
211 between 580 °C and 699 °C with a total mass loss of 0.24%. This could be the dehydroxylation

212 of illite and montmorillonite which are typically dehydroxylated between 550 °C and 880 °C.
213 There is, however, no change in structure for illite and montmorillonite after dehydroxylation.
214
215 FTIR absorption spectra of the calcined clay samples are shown in Figure 6. The absorption
216 band at 3694 cm⁻¹ signifies that kaolinite is present and can be traced to the vibration of inner-
217 surface OH groups. The absorption band at 3619 cm⁻¹ that is also assigned to the stretching of
218 inner-surface hydroxyl groups relates to smectite or illite. As temperature drops, the band at
219 1470 cm⁻¹ loses strength and gradually falls until it eventually vanishes at 1000 °C which is
220 attributed to the transformation of smectite and illite. The stretching and distortion of water
221 molecules caused by OH is what causes the bands at 911, 778, and 688 cm⁻¹, which get smaller
222 as the temperature rises.

223

224 *Effect on compressive strength*

225 Figure 7 presents the development of compressive strengths of the composite cement mortars
226 with reference to the control mortar after 91 days curing. At 3 and 7 days, all the calcined clay
227 blended cements recorded strengths lower than the reference cement which significantly
228 improved after 28 days of curing. It was also observed that, compressive strength for the
229 reference cement did not appreciate significantly after 91 days curing. Calcined clay blended
230 cements, on the other hand, were seen to exhibit appreciable strength gains, with 900 °C
231 obtaining similar results as the reference cement. The performance of the calcined clay at later
232 ages can possibly be due to improved particle packing in the cement system with calcined clay
233 having the lowest median particle size. Also, at later ages, pozzolanic reactivity is more likely
234 to increase due to the continuous consumption of Ca(OH)₂ by the constituents of the calcined
235 clay, as curing age increases, to produce extra calcium silicate hydrates needed for strength
236 development.

237

238 *Effect of calcination temperature on pozzolanic reactivity*

239 Frattini test results showing the pozzolanic reactivity of the calcined clay is presented in
240 Figures 8 and 9. All the calcined clay samples were found above the lime solubility curve at 3
241 days. This indicates that the calcined clay samples showed no significant pozzolanic reactivity
242 at this point. In Figure 8, the pastes which had clays treated at 700 °C, 900 °C and 1000 °C
243 were found at the lower side of the solubility curve. This confirms the consumption of Ca(OH)_2
244 by the constituents of the cement, thereby proving pozzolanicity of these calcined clays. Even
245 though clays calcined at 600 and 1000 °C were found above the curve, their position, with
246 respect to the curve, after 28 days confirms some amount of reactivity, however slow.

247

248 The consumption of Ca(OH)_2 at various curing times, derived from the TGA data after the
249 portlandite consumption test is shown in Figure 10. The highest consumption per mass was
250 seen in clays calcined at 900 °C and 800 °C and 700 °C, in increasing order of reactivity. It
251 was also observed that portlandite consumption in all test materials increased with increasing
252 curing time. As expected, silica sand, which served as a reference material, recorded the lowest
253 reactivity.

254

255 Figure 11 presents the SAI results, computed from the compressive strength data. At 28 days,
256 apart from 600 °C and 1000 °C which fell short of the ASTM minimum requirement of 75%,
257 the SAI of all other samples were found to be within acceptable limits of pozzolanic reactivity.
258 SAI at 91 days showed significant improvement, with 600 °C and 1000 °C obtaining figures
259 above the minimum 75%. Results of the relative strength index have also been presented in
260 Figure 12. Samples containing clay calcined at 600 °C and 1000 °C showed negative RSI at 3,
261 7 and 28 days. This is an indication that the contribution of the 20% calcined clay was inferior

262 to cement. 700 °C, 800 °C and 900 °C showed positive RSI values which indicates that their
263 contribution to pozzolanic reactivity is appreciable and is likely to overcome dilution effect. It
264 can be inferred from the findings of SAI and RSI that the ideal calcination temperature falls
265 between 800-900 °C.

266

267 *Effect of calcined clay on hydration products*

268 Figure 13 displays the XRD patterns of hydrated blended cement paste incorporated with 20%
269 calcined at various temperatures. Portlandite, denoted by CH, was observed in both the
270 reference sample and the blended mortars. As seen, the portlandite peaks in the blended cement
271 samples were shorter than that of the reference cement paste. The intensities of these peaks,
272 except 1000 °C, were seen to decrease with increasing calcining temperatures. This observation
273 is similar to the findings of Du and Pang (2018). The lowered portlandite peak intensities are
274 as a result of pozzolanic reactivity of the calcined clay samples, consuming the $\text{Ca}(\text{OH})_2$
275 released from the hydration process. Again, the replacement of 20% cement with calcined clay
276 reduced the quantity of cement and consequently reduced the production of portlandite.
277 Furthermore, substantial part of portlandite is likely to go into reaction with SiO_2 from the
278 calcined clay to produce further cementitious compounds such as C-S-H.

279

280 **Conclusion**

281 This investigation has studied the mineralogical, pozzolanic reactivity and mechanical
282 performance of low-grade kaolinitic clay (calcined at varying temperatures) in Portland cement
283 mortar and the following conclusions drawn:

- 284 1. From the DSC results, kaolinite underwent partial dehydroxylation at 600 °C to generate
285 metakaolin and at 700 °C, complete dehydration was achieved. The crystallinity of the clay
286 was slowly reduced, giving way to the emergence of amorphous phases, after calcining at

287 varying temperatures. Due to recrystallization and a decrease in specific surface area,
288 pozzolanic activity was reduced at a temperature of 1000 °C.

289 2. The partial replacement of cement with calcined clay caused a reduction in early strength
290 but increased noticeably at 91 days. Water demand, as well as setting time decreased with
291 increasing calcination temperature.

292 3. Frattini test revealed minimal pozzolanic reactivity at 600 °C and 1000 °C. This trend was
293 confirmed by the portlandite consumption test, strength activity index (SAI) and the relative
294 strength index (RSI).

295 4. XRD studies revealed the consumption of Portlandite after 28 days hydration of blended
296 calcined clay-Portland cement paste. Excess $\text{Ca}(\text{OH})_2$ was seen in samples containing 1000
297 °C calcined clay, confirming low pozzolanic reactivity.

298 5. Considering the thermogravimetric, pozzolanic reactivity and mechanical properties, the
299 most effective calcination temperature was found between 800 and 900 °C.

300

301 **Data Availability Statement**

302 Some or all data, models, or code that support the findings of this study are available from the
303 corresponding author upon reasonable request.

304

305 **References**

306 Alujas, A., Fernández, R., Quintana, R., Scrivener, K.L., Martirena, F., 2015. Pozzolanic
307 reactivity of low grade kaolinitic clays: Influence of calcination temperature and impact of
308 calcination products on OPC hydration. *Appl. Clay. Sci.*, 94-101

309 Antoni, M., Rossen, J., Martirena, F., Scrivener, K., 2012. Cement substitution by a
310 combination of metakaolin and limestone. *Cem. Concr. Res.* 12, 1579-1589

311 Aprianti S, E., 2017. A huge number of artificial waste material can be supplementary
312 cementitious material (SCM) for concrete production – a review part II. *J. Clean. Prod.*,
313 4178-4194

- 314 Arslan, F., Benli, A., Karatas, M., 2020. Effect of high temperature on the performance of
315 self-compacting mortars produced with calcined kaolin and metakaolin. *Constr. Build.*
316 *Mater.*, 119497
- 317 Boakye, K., Khorami, M., Saidani, M., Ganjian, E., Dunster, A., Ehsani, A., Tyrer, M., 2022.
318 Mechanochemical characterisation of calcined impure kaolinitic clay as a composite binder in
319 cementitious mortars. *Journal of Composites Science*. 134
- 320 Cardinaud, G., Rozière, E., Martinage, O., Loukili, A., Barnes-Davin, L., Paris, M., Deneele,
321 D., 2021. Calcined clay – Limestone cements: Hydration processes with high and low-grade
322 kaolinite clays. *Constr. Build. Mater.*, 122271
- 323 Chakchouk, A., Trifi, L., Samet, B., Bouaziz, S., 2009. Formulation of blended cement:
324 Effect of process variables on clay pozzolanic activity. *Constr. Build. Mater.* 3, 1365-1373
- 325 Dixit, A., Du, H., Pang, S.D., 2021. Performance of mortar incorporating calcined marine
326 clays with varying kaolinite content. *J. Clean. Prod.*, 124513
- 327 Dixit, A., Du, H., Pang, S.D., 2020. Marine clay in ultra-high performance concrete for filler
328 substitution. *Constr. Build. Mater.*, 120250
- 329 Du, H., Pang, S.D., 2018. Value-added utilization of marine clay as cement replacement for
330 sustainable concrete production. *J. Clean. Prod.*, 867-873
- 331 El-Diadamony, H., Amer, A.A., Sokkary, T.M., El-Hoseny, S., 2018. Hydration and
332 characteristics of metakaolin pozzolanic cement pastes. *HBRC Journal*. 2, 150-158
- 333 Ferreira, S., Herfort, D., Damtoft, J.S., 2017. Effect of raw clay type, fineness, water-to-
334 cement ratio and fly ash addition on workability and strength performance of calcined clay –
335 Limestone Portland cements. *Cem. Concr. Res.*, 1-12
- 336 He, C., Makovicky, E., Osbæck, B., 1994. Thermal stability and pozzolanic activity of
337 calcined kaolin. *Appl. Clay. Sci.* 3, 165-187
- 338 Hollanders, S., Adriaens, R., Skibsted, J., Cizer, Ö, Elsen, J., 2016. Pozzolanic reactivity of
339 pure calcined clays. *Appl. Clay. Sci.*, 552-560
- 340 Huang, W., Kazemi-Kamyab, H., Sun, W., Scrivener, K., 2017. Effect of replacement of
341 silica fume with calcined clay on the hydration and microstructural development of eco-
342 UHPFRC. *Mater Des*, 36-46
- 343 Jafari, K., Rajabipour, F., 2020. Performance of Impure Calcined Clay as a Pozzolan in
344 Concrete. *Transport Research Record*. 2, 643-645
- 345 Jafari, K., Rajabipour, Farshad, 2020. Performance of Impure Calcined Clay as a Pozzolan in
346 Concrete. *Transportation Research Record: Journal of Transportation Research Board*. 2, 98-
347 107
- 348 Juenger, M.C.G., Siddique, R., 2015. Recent advances in understanding the role of
349 supplementary cementitious materials in concrete. *Cem. Concr. Res.*, 71-80

- 350 Juenger, M.C.G., Snellings, R., Bernal, S.A., 2019. Supplementary cementitious materials:
351 New sources, characterization, and performance insights. *Cem. Concr. Res.*, 257-273
- 352 Kaminskas, R., Barauskas, I., Laskevicius, K., 2023. Improvement of the Pozzolanitic
353 Properties of Calcined Mica Clay. *J. Mater. Civ. Eng.* 1, 04022373
- 354 Kang, S., Kwon, Y., Moon, J., 2022. Influence of calcination temperature of impure
355 kaolinitic clay on hydration and strength development of ultra-high-performance
356 cementitious composite. *Constr. Build. Mater.*, 126920
- 357 Karatas, M., Benli, A., Arslan, F., 2020. The effects of kaolin and calcined kaolin on the
358 durability and mechanical properties of self-compacting mortars subjected to high
359 temperatures. *Constr. Build. Mater.*, 120300
- 360 Kovářík, T., Bělský, P., Novotný, P., Říha, J., Savková, J., Medlín, R., Rieger, D., Holba, P.,
361 2015. Structural and physical changes of re-calcined metakaolin regarding its reactivity.
362 *Constr. Build. Mater.*, 98-104
- 363 McCarthy, M.J., Robl, T., Csetenyi, L.J., 2017. 14 - Recovery, processing, and usage of wet-
364 stored fly ash, in: Robl, T., Oberlink, A., Jones, R. (Eds.), *Coal Combustion Products*
365 (CCP's). Woodhead Publishing, pp. 343-367
- 366 Msinjili, N.S., Gluth, G.J.G., Sturm, P., Vogler, N., Kune, H., 2019. Comparison of calcined
367 illitic clays (brick clays) and lowgrade kaolinitic clays as supplementary cementitious
368 materials. *Materials and Structures.* 94
- 369 Scrivener, K., Martirena, F., Bishnoi, S., Maity, S., 2018. Calcined clay limestone cements
370 (LC3). *Cem. Concr. Res.*, 49-56
- 371 Seiffarth, T., Hohmann, M., Posern, K., Kaps, C., 2013. Effect of thermal pre-treatment
372 conditions of common clays on the performance of clay-based geopolymeric binders. *Appl.*
373 *Clay. Sci.*, 35-41
- 374 Siddika, A., Mamun, M.A.A., Alyousef, R., Mohammadhosseini, H., 2020. State-of-the-art-
375 review on rice husk ash: A supplementary cementitious material in concrete. *Journal of King*
376 *Saud University - Engineering Sciences*
- 377 Taylor-Lange, S.C., Lamon, E.L., Riding, K.A., Juenger, M.C.G., 2015. Calcined kaolinite-
378 bentonite clay blends as supplementary cementitious materials. *Appl. Clay. Sci.*, 84-93
- 379 Thapa, V.B., Waldmann, D., Simon, C., 2019. Gravel wash mud, a quarry waste material as
380 supplementary cementitious material (SCM). *Cem. Concr. Res.*, 105833
- 381 Tironi, A., Scian, A.N., Irassar, E.F., 2017. Blended cements with limestone filler and
382 kaolinitic calcined clay: Filler and pozzolanitic effects. *J. Mater. Civ. Eng.* 9, 04017116
- 383 Tironi, A., Trezza, M.A., Scian, A.N., Irassar, E.F., 2013. Assessment of pozzolanitic activity
384 of different calcined clays. *Cement and Concrete Composites*, 319-327

- 385 Zhao, D., Khoshnazar, R., 2020. Microstructure of cement paste incorporating high volume
386 of low-grade metakaolin. *Cement and Concrete Composites*, 103453
- 387 Zheng, D., Liang, X., Cui, H., Tang, W., Liu, W., Zhou, D., 2022. Study of performances and
388 microstructures of mortar with calcined low-grade clay. *Constr. Build. Mater.*, 126963
- 389 Zhou, D., Wang, R., Tyrer, M., Wong, H., Cheeseman, C., 2017. Sustainable infrastructure
390 development through use of calcined excavated waste clay as a supplementary cementitious
391 material. *J. Clean. Prod.*, 1180-1192
- 392 Zhou, Y., Zhang, Z., 2020. Effect of fineness on the pozzolanic reaction kinetics of slag in
393 composite binders: Experiment and modelling. *Constr. Build. Mater.*, 121695
- 394
395
- 396 Antoni, M., Rossen, J., Martirena, F., Scrivener, K., 2012. Cement substitution by a
397 combination of metakaolin and limestone. *Cem. Concr. Res.* 12, 1579-1589
- 398 Arslan, F., Benli, A., Karatas, M., 2020. Effect of high temperature on the performance of
399 self-compacting mortars produced with calcined kaolin and metakaolin. *Constr. Build.*
400 *Mater.*, 119497
- 401 Danner, T., Norden, G., Justnes, H., 2018. Characterisation of calcined raw clays suitable as
402 supplementary cementitious materials. *Appl. Clay. Sci.*, 391-402
- 403 Dixit, A., Du, H., Pang, S.D., 2021. Performance of mortar incorporating calcined marine
404 clays with varying kaolinite content. *J. Clean. Prod.*, 124513
- 405 Dixit, A., Du, H., Pang, S.D., 2020. Marine clay in ultra-high performance concrete for filler
406 substitution. *Constr. Build. Mater.*, 120250
- 407 Du, H., Pang, S.D., 2018. Value-added utilization of marine clay as cement replacement for
408 sustainable concrete production. *J. Clean. Prod.*, 867-873
- 409 Ferreira, S., Herfort, D., Damtoft, J.S., 2017. Effect of raw clay type, fineness, water-to-
410 cement ratio and fly ash addition on workability and strength performance of calcined clay –
411 Limestone Portland cements. *Cem. Concr. Res.*, 1-12
- 412 He, C., Makovicky, E., Osbæck, B., 1994. Thermal stability and pozzolanic activity of
413 calcined kaolin. *Appl. Clay. Sci.* 3, 165-187
- 414 Kaminskas, R., Barauskas, I., Laskevicius, K., 2023. Improvement of the Pozzolanic
415 Properties of Calcined Mica Clay. *J. Mater. Civ. Eng.* 1, 04022373
- 416 Kang, S., Kwon, Y., Moon, J., 2022. Influence of calcination temperature of impure
417 kaolinitic clay on hydration and strength development of ultra-high-performance
418 cementitious composite. *Constr. Build. Mater.*, 126920

419 Karatas, M., Benli, A., Arslan, F., 2020. The effects of kaolin and calcined kaolin on the
420 durability and mechanical properties of self-compacting mortars subjected to high
421 temperatures. *Constr. Build. Mater.*, 120300

422 Lothenbach, B., Scrivener, K., Hooton, R.D., 2011. Supplementary cementitious materials.
423 *Cem. Concr. Res.* 12, 1244-1256

424 Msinjili, N.S., Gluth, G.J.G., Sturm, P., Vogler, N., Kune, H., 2019. Comparison of calcined
425 illitic clays (brick clays) and lowgrade kaolinitic clays as supplementary cementitious
426 materials. *Materials and Structures.* 94

427 Scrivener, K., Martirena, F., Bishnoi, S., Maity, S., 2018. Calcined clay limestone cements
428 (LC3). *Cem. Concr. Res.*, 49-56

429 Snellings, R., Cizer, Ö, Horckmans, L., Durdziński, P.T., Dierckx, P., Nielsen, P., Van Balen,
430 K., Vandewalle, L., 2016. Properties and pozzolanic reactivity of flash calcined dredging
431 sediments. *Appl. Clay. Sci.*, 35-39

432 Taylor-Lange, S.C., Lamon, E.L., Riding, K.A., Juenger, M.C.G., 2015. Calcined kaolinite–
433 bentonite clay blends as supplementary cementitious materials. *Appl. Clay. Sci.*, 84-93

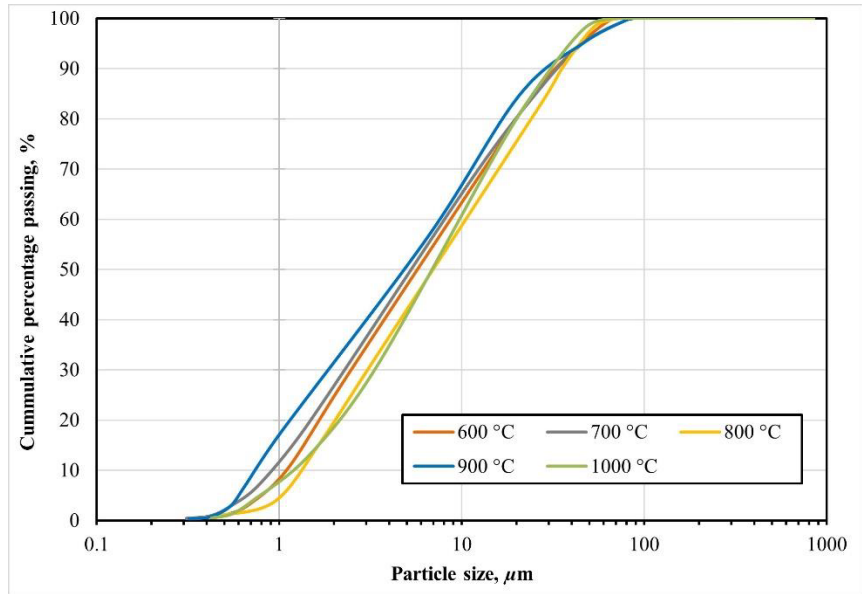
434 Tironi, A., Scian, A.N., Irassar, E.F., 2017. Blended cements with limestone filler and
435 kaolinitic calcined clay: Filler and pozzolanic effects. *J. Mater. Civ. Eng.* 9, 04017116

436 Zheng, D., Liang, X., Cui, H., Tang, W., Liu, W., Zhou, D., 2022. Study of performances and
437 microstructures of mortar with calcined low-grade clay. *Constr. Build. Mater.*, 126963

438 Zhou, D., Wang, R., Tyrer, M., Wong, H., Cheeseman, C., 2017. Sustainable infrastructure
439 development through use of calcined excavated waste clay as a supplementary cementitious
440 material. *J. Clean. Prod.*, 1180-1192

441 .

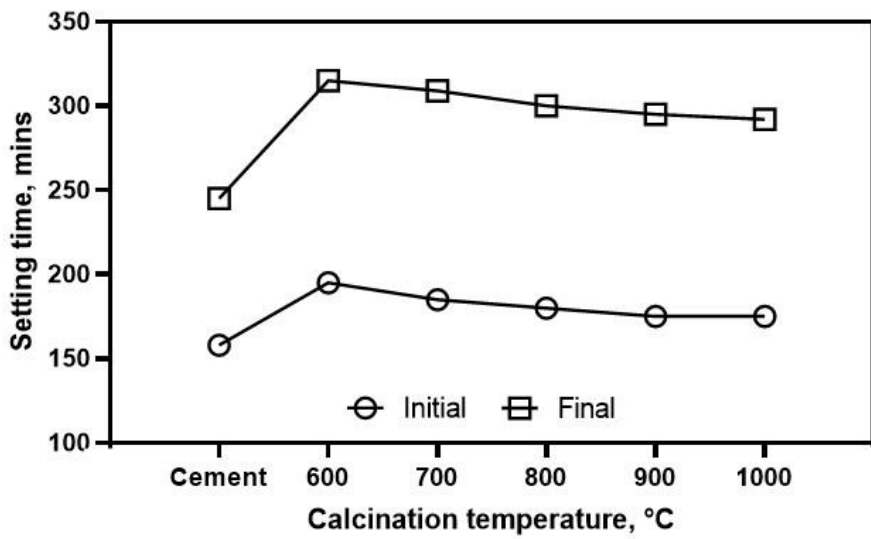
442



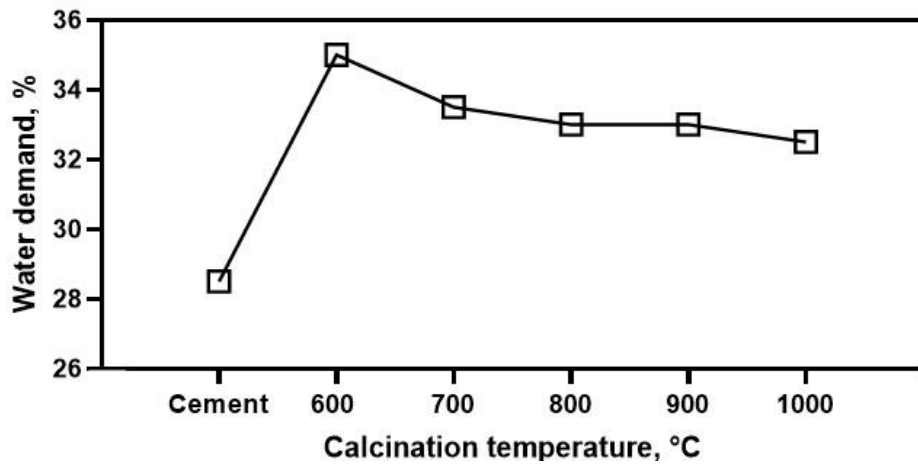
443

444

Fig. 1. Particle size distribution of clay calcined at varying temperatures.

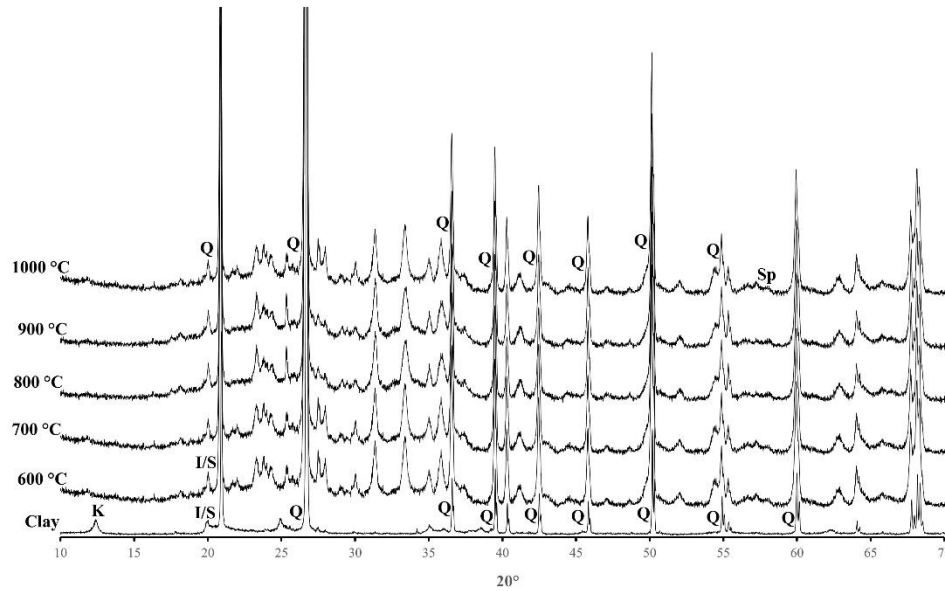


445

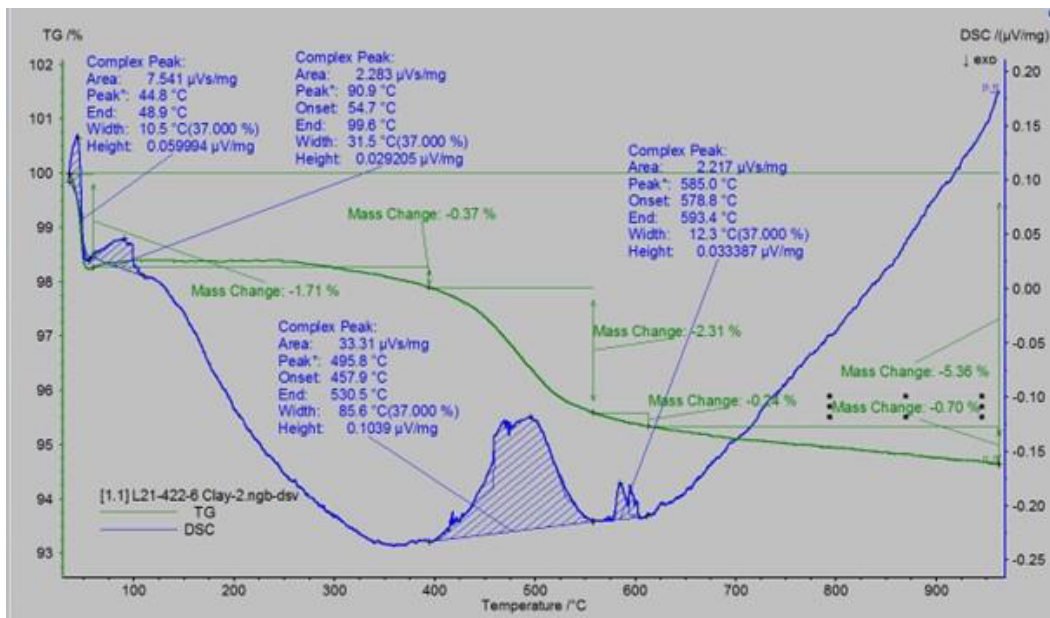


446

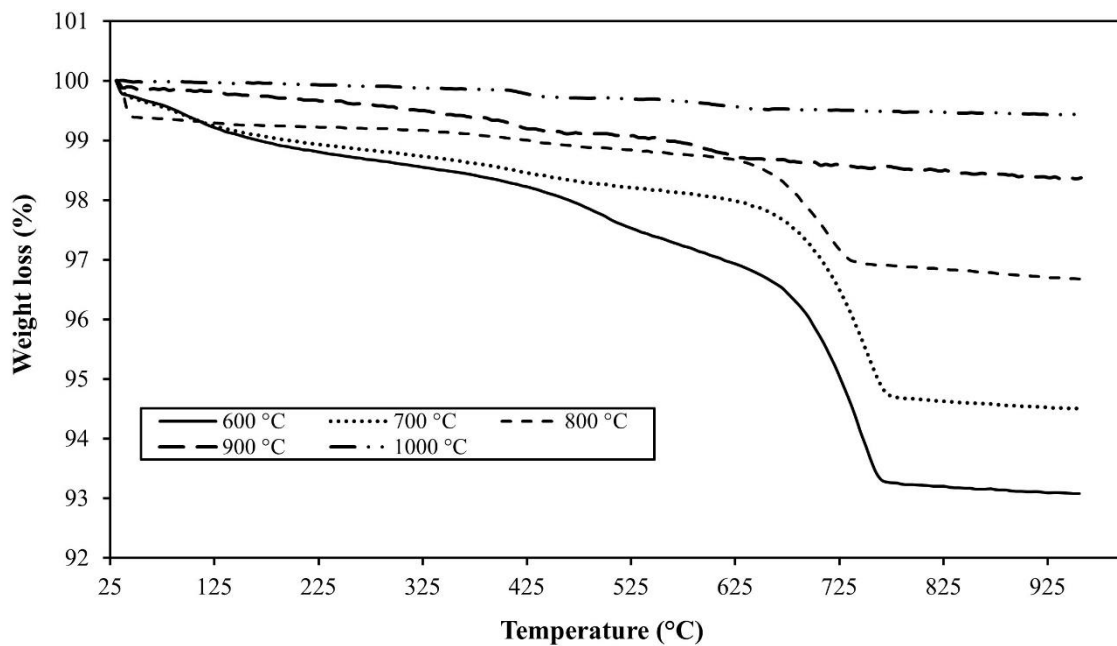
447 **Fig. 2.** Setting time (a) and water demand (b) of CEM I and paste containing calcined clay of
 448 different temperatures.



449
 450 **Fig. 3.** XRD pattern of raw and calcined clays (K: Kaolinite; I: Illite; S: Smectite; Q: Quartz;
 451 Sp: Spinel).



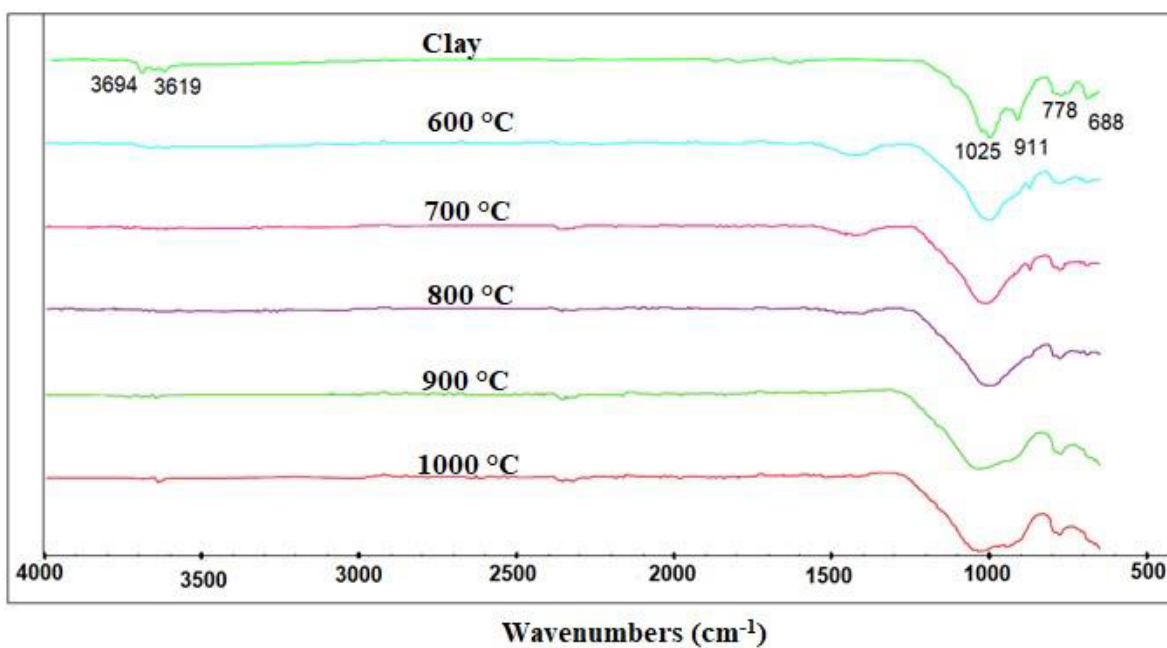
452
 453 **Fig. 4.** TG/DSC of raw clay



454

455

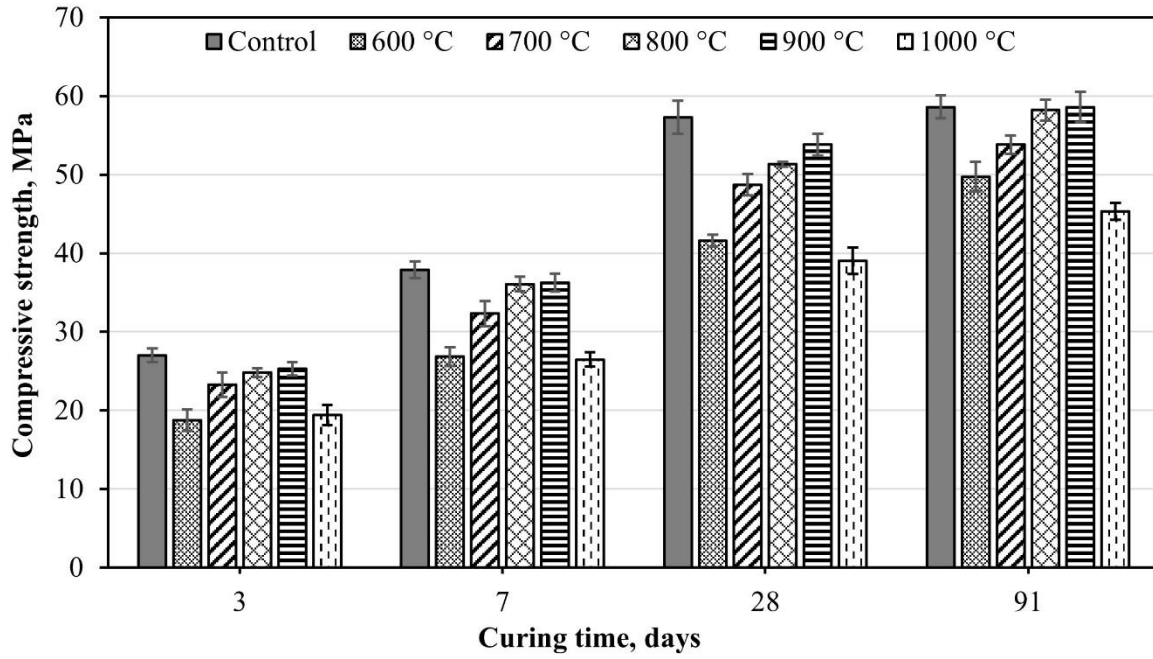
Fig. 5. Thermogravimetric analysis of calcined clays.



456

457

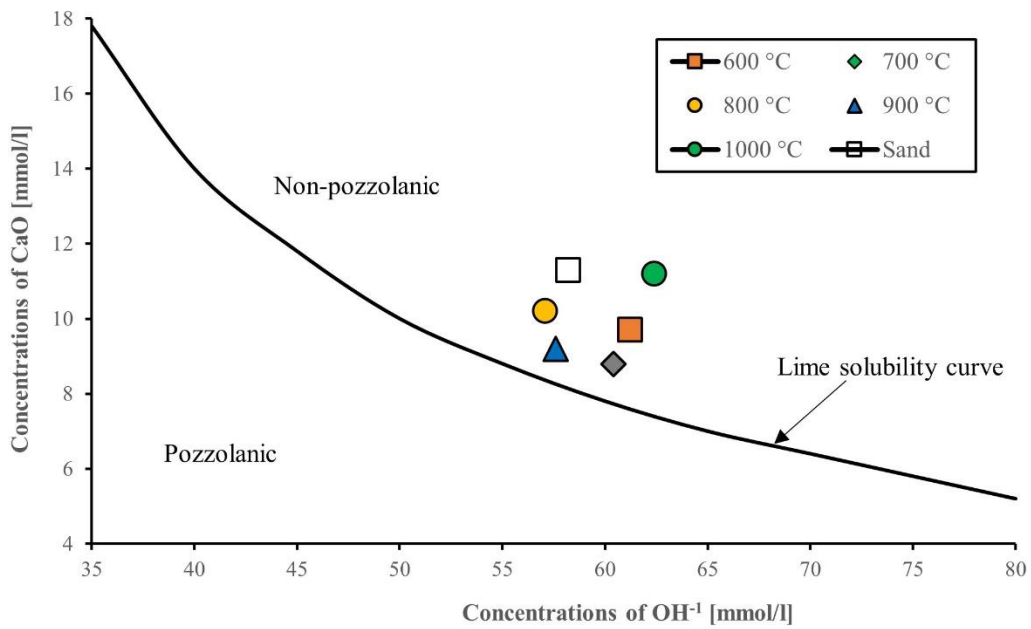
Fig. 6. FTIR patterns of calcined clays.



458

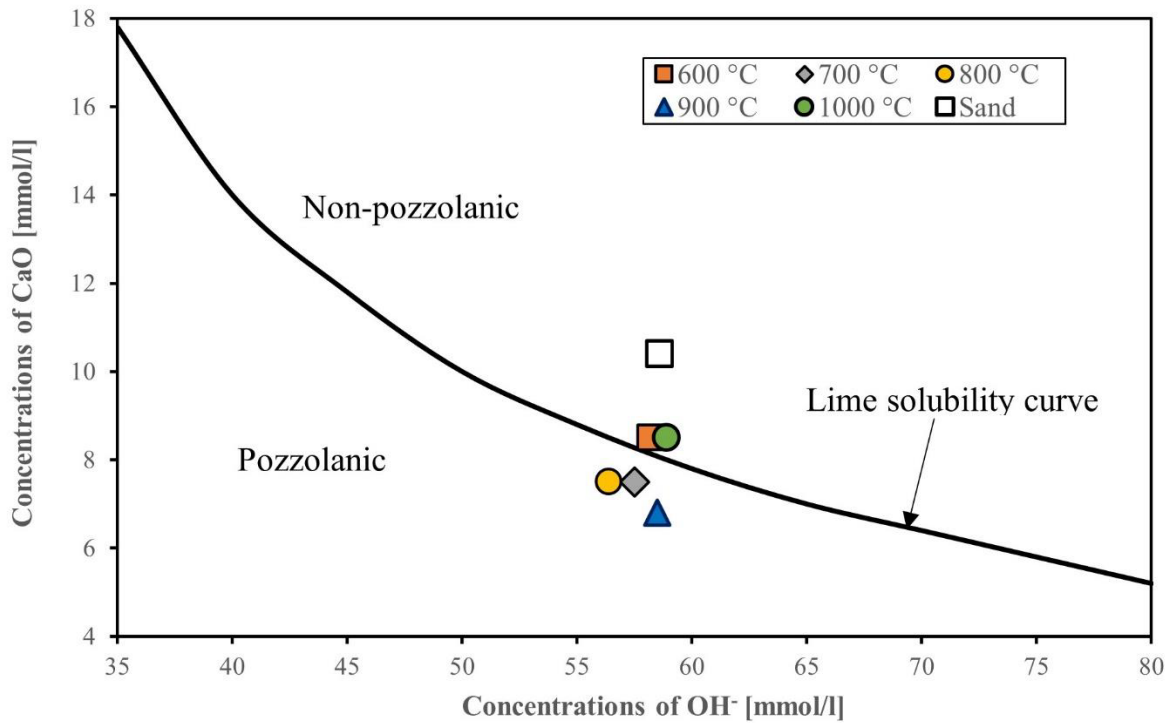
459 **Fig. 7.** Compressive strength development of blended cement containing clay calcined at
 460 varying temperatures.

461



462

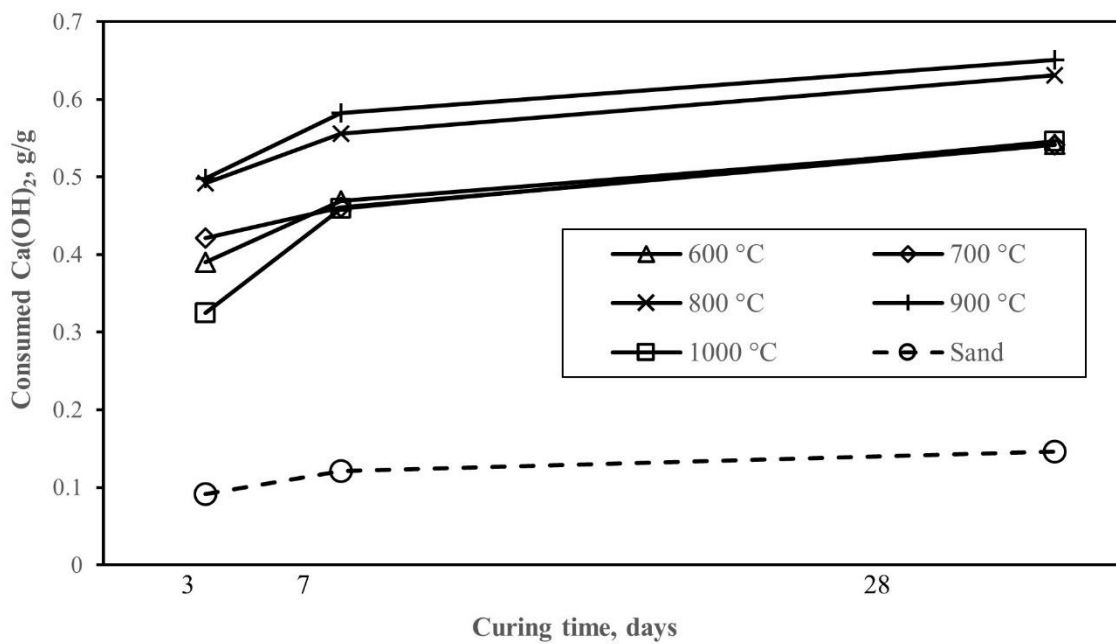
463 **Fig. 8.** Frattini test showing reactivity of calcined clay at 3 days.



464

465

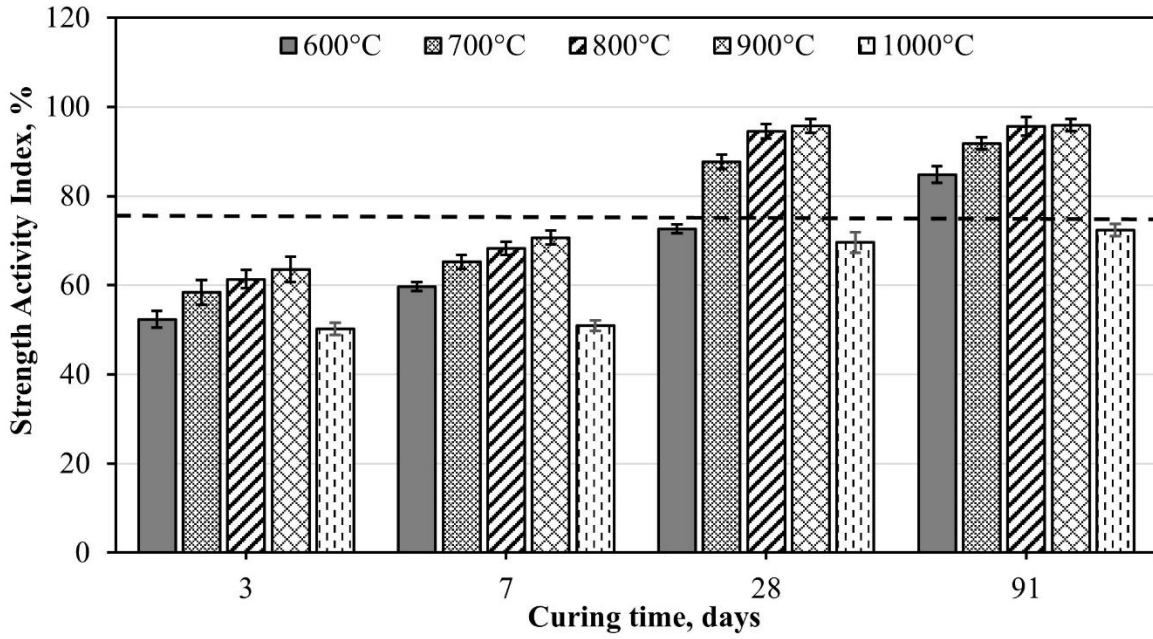
Fig. 9. Frattini test showing reactivity of calcined clay at 28 days.



466

467

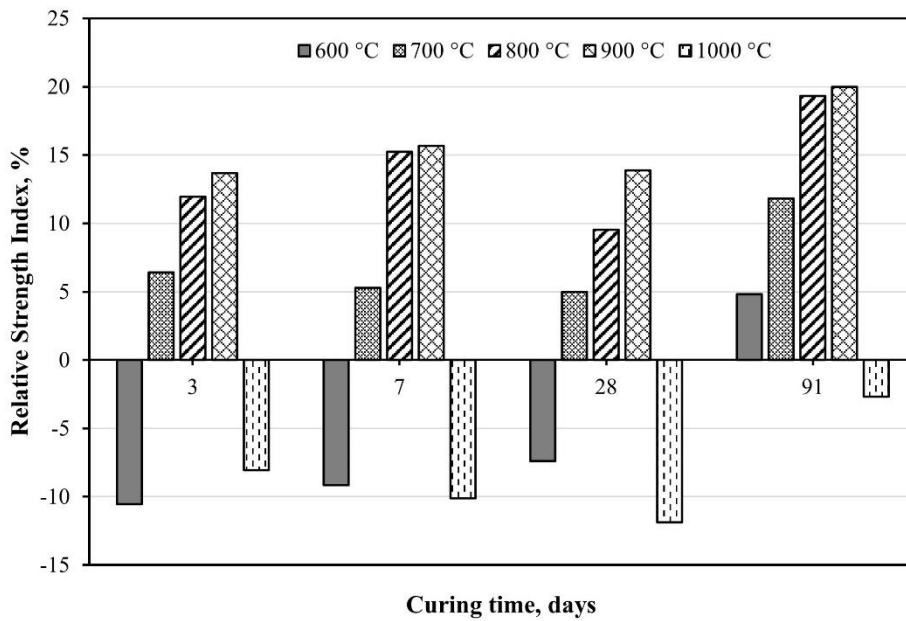
Fig. 10. Portlandite consumption of calcined clay samples



468

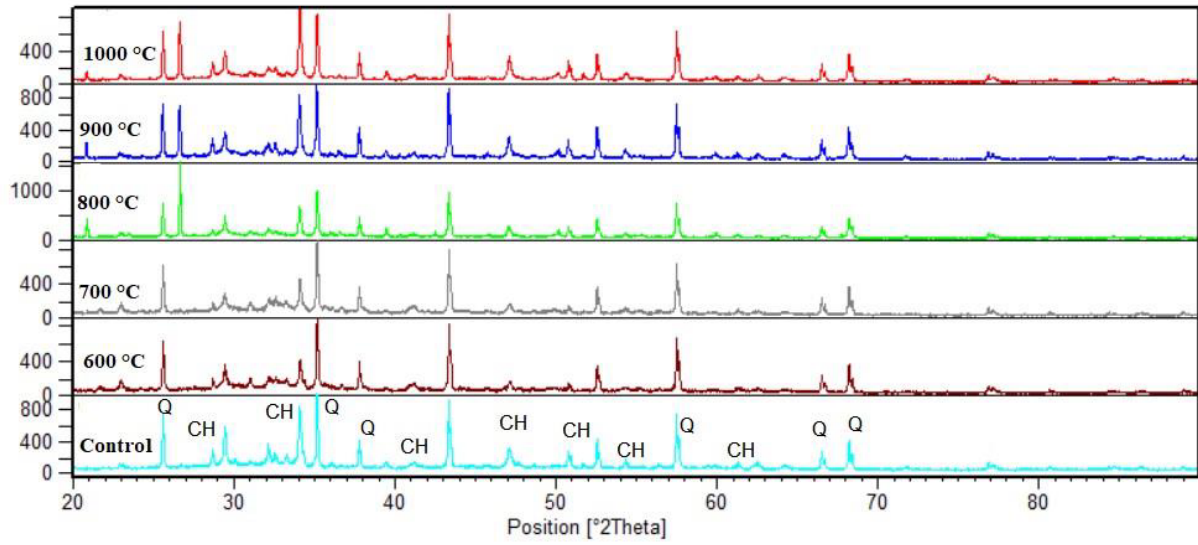
469 **Fig. 11.** Strength activity index (SAI) of mortar containing 20% calcined clay at varying
 470 temperatures.

471



472

473 **Fig. 12.** Relative strength index (RSI) of mortar containing 20% calcined clay at varying
 474 temperatures.



475

476

Fig. 13. XRD pattern of cement paste containing 20% calcined clays of different calcination temperatures and cured for 28 days.

477

478

479

480

481

482

483

484

485

486

487